Authors' responses to reviewers' comments for the paper wes-2025-240 "Integrated Control of Floating Offshore Wind Farms with Reconfigurable Layouts"

Yue Niu and Ryozo Nagamune

January 19, 2026

We would like to thank reviewers for their careful reviews and valuable comments, which were taken into consideration in revising and improving the paper. Based on the comments and suggestions, we have made major revisions of the manuscript and highlighted the revised parts with red color. Below, please find our responses to each reviewer.

Note 1: Positive comments are omitted; thank you for those encouraging comments.

Note 2: Added references are given at the end of this document. Reference numbers are valid only in this document; references in the revised manuscript appear in the format of the journal.

Responses to Reviewer 1

General comments

1. **Comment:** *Several important methodological details are currently missing or underdeveloped. Because the study relies heavily on FLORIS, the paper would benefit from a description of the chosen velocity, deflection, and turbulence models, along with the parameters used and the motivation for selecting them. These aspects have a strong influence on the results, and clarifying them would greatly strengthen the robustness and reproducibility of the findings.*

   Response: Thank you very much for this comment. We have updated the manuscript to explicitly describe the wake models (velocity deficit, deflection, turbulence, combination) used in our study in Section 3.2.2 as follows.

   Change in manuscript:

   In this study, wake effects in FLORIS are represented by four submodels, each used with the default parameter values provided by FLORIS [1]:

   - **Velocity deficit model:** For the wake velocity deficit, we use the empirical Gaussian wake model, which assumes a Gaussian distribution of the velocity deficit [2, 3].
   - **Wake deflection model:** Wake deflection is computed using FLORIS's empirical Gaussian deflection model based on yaw-misalignment wake-deflection formulations [2, 3].
   - **Wake turbulence model:** To account for added turbulence in turbine wakes, we employ the wake-induced mixing model in FLORIS, which generalizes wake-added turbulence in the empirical Gaussian wake model [4]. In this model, upstream turbines

contribute to mixing in the flow, yielding a wake-induced mixing factor that is passed to the velocity deficit and wake deflection models to modify the wake width and the wake-centerline deflection, respectively.

- **Wake combination model:** Wake effects from multiple turbines are combined using the sum-of-squares freestream superposition model [5].

2. **Comment:** *The implementation of wake mixing is not fully specified. For example, if the Helix model introduced recently in FLORIS is used, details such as the chosen amplitude and the rationale behind it would be valuable.*

   Response: Thank you for this important comment. We agree that the original manuscript did not describe the wake-mixing implementation with sufficient clarity. We have revised the manuscript as follows.

   Change in manuscript:

   - **Abstract:** revised to explicitly list the coordinated control methods:
     The framework coordinates four farm-level control strategies, that is, turbine repositioning, wake steering, power derating, and Helix wake mixing, to either (i) maximize total farm power output or (ii) track a prescribed farm-level power setpoint while mitigating wake effects.
   - **Introduction:** added sentences defining terminology:
     In this paper, "dynamic wake mixing" refers to Helix wake mixing realized via periodic individual-blade pitch excitation.
   - **Section 3.1:** revised to define the wake-mixing parameter clearly:
     where θ_i (deg) is ..., and $\beta_{\mathrm{amp},i}$ (deg) is the mean-to-peak amplitude of the sinusoidal blade-pitch excitation used for Helix wake mixing at turbine i ($i = 1, \ldots, N$).
   - **Section 3.1.2:** clarified the Helix-mode implementation and parametrization:
     In this study, wake mixing is realized using FLORIS's Helix mode (periodic individual blade-pitch actuation), with the wake-mixing intensity parameterized by the mean-to-peak excitation amplitude β_{amp} (van den Berg et al., 2024, [6, 7, 8]).
   - **Section 3.2.2:** added a clarification of the wake-mixing implementation:
     Helix wake mixing is represented using FLORIS's built-in active wake control "helix" operation model, which parameterizes the time-averaged impact of helix pitch excitation on turbine power/thrust and wake recovery and has been calibrated in FLORIS as a standalone wake-mixing representation.
   - **Section 4.1:** added a clarification of the selected maximum mean-to-peak amplitude:
     The Helix excitation amplitude is bounded to $\beta_{\mathrm{amp},i} \in [0, 5]$ degrees, where $\beta_{\mathrm{amp},i} = 0$ corresponds to no wake-mixing actuation and the upper bound is consistent with excitation levels reported in prior studies (e.g., up to 4 degrees in van den Berg et al., 2024, and up to 5 degrees in [6]).

3. **Comment:** *The interaction between wake steering and curtailment could also be discussed more explicitly, especially given the complex aerodynamic behavior associated with simultaneous misalignment and changes in thrust coefficient.*

Moreover, there is no mention of how curtailment is performed, which is rather crucial because it determines how the thrust coefficient changes.

It is also not clear whether the authors are combining wake mixing and wake steering simultaneously. Although this could be possible in FLORIS, there has not been a validation of the results yet. The effects on the wake do not simply sum up, and this would likely result in a critical overprediction of power.

Response: Thank you for raising these important points. We have revised the manuscript to (i) more explicitly discuss the interaction between wake steering and power derating/wake mixing, (ii) clarify how these control actions are implemented in FLORIS (including how derating modifies thrust), and (iii) clearly state the modeling assumptions and limitations associated with their combined application. These revisions have been added to Section 3.2.2 as follows.

Changes in manuscript:

The wind farm control methods are implemented in FLORIS through the control inputs $\mathbf{U}$ as follows:

- **Wake steering:** Wake steering is implemented by prescribing yaw misalignment commands θ_i, which modify turbine power/thrust and the resulting wake deflection in a steady-state sense.
- **Turbine repositioning:** Turbine repositioning is represented by the same yaw commands θ_i but is coupled with a steady-state turbine position solver (see Sect. 3.2.4) that enforces static equilibrium between aerodynamic loading and mooring restoring forces to update the turbine positions. The updated positions are then evaluated in FLORIS, thereby changing wake overlap and farm performance.
- **Power derating:** Power derating is implemented by prescribing a per-turbine power cap $P_{\text{set},i}$. This setpoint is passed to FLORIS's "simple-derating" turbine operation model, which first evaluates the turbine power P_i and thrust coefficient from the power-thrust table at the local inflow and then enforces the cap as $P_i = \min\{P_i, P_{\text{set},i}\}$. When the cap limits the power output, FLORIS reduces the turbine thrust coefficient accordingly to reflect the curtailed operating point.
- **Helix wake mixing:** Helix wake mixing is represented using FLORIS's built-in active wake control "helix" operation model, which parameterizes the time-averaged impact of helix pitch excitation on turbine power/thrust and wake recovery and has been calibrated in FLORIS as a standalone wake-mixing representation.

It should be noted that FLORIS has not yet been extensively validated for cases in which a turbine is simultaneously yaw-misaligned and operated in either derated mode or active wake-mixing mode. In our optimization framework, we nevertheless allow yaw misalignment to be applied concurrently with either power derating or Helix wake mixing for each turbine. Under such combined operation, FLORIS predicts steady-state changes in turbine power/thrust, wake deflection, and wake recovery; however, the corresponding results should be interpreted with this validation limitation in mind. Moreover, when wake steering and power derating/Helix wake mixing are applied simultaneously, yaw-induced power loss is not captured (as observed in our simulations) in the FLORIS prediction; therefore, to avoid overestimating power capture under yaw misalignment, we apply a yaw-power loss correction for yawed turbines, $P_i \leftarrow P_i(\cos\theta_i)^{p_P}$, with a parameter value $p_P = 1.88$ [9]. For yaw-only wake-steering/turbine-repositioning cases, we do not apply this additional correction to avoid double counting.

4. **Comment:** *Another point concerns the ambient conditions used in the simulations, such as turbulence intensity and vertical shear. These are key inputs to FLORIS and strongly influence wake recovery, so specifying them would improve transparency.*

   Response: Thank you for this helpful comment. We revised the manuscript to report the turbulence intensity, vertical shear, and wind veer in Section 4.2.1 as follows.

   Change in manuscript:

   All simulations assume an ambient turbulence intensity of 0.06, a power-law vertical shear exponent of 0.12, and zero wind veer.

5. **Comment:** *Overall, I believe that the results may not be reliable without a clear justification for the modeling choices. With a more complete description of the methodology and modeling assumptions, the results would become more reliable and easier for readers to interpret and reproduce.*

   Response and Change in manuscript: Thank you for this important comment. In response, we strengthened the methodology description and clarified the key modeling assumptions to improve transparency, reproducibility, and interpretation of the results. Please see our responses to all the comments.

6. **Comment:** *If the authors are able to incorporate the suggested methodological clarifications, it could also be beneficial to expand the Results section. At present, the analysis feels somewhat limited, and given that the authors have developed a promising control framework, there is an opportunity to demonstrate its capabilities more extensively.*

   Response and Change in manuscript: Thank you for this helpful suggestion. In response, we expanded the Results section with:

   - additional benchmark results to isolate the effect of turbine repositioning together with wake steering (Figs. 7-8),
   - visualization of the local turbine inflow velocities in the Results figures (Figs. 9-10),
   - more elaborate, self-contained figure captions throughout the Results section, and
   - expanded discussion accompanying each figure that clearly states what is shown and the main conclusions supported by each figure.

Specific comments

1. **Comment:** *Line 52: the references for wake mixing could be updated to include more recent work.*

   Response: Thank you for this comment. We added more recent references [6, 7, 8] on wake mixing in Introduction.

   Change in manuscript:

   To overcome this limitation, turbine repositioning can be integrated with ... and dynamic wake mixing (Goit and Meyers, 2015; van den Berg et al., 2024; [6, 7, 8]).

2. **Comment:** *Line 56: a short discussion of how wake mixing can be implemented, with examples from the literature, would be helpful.*

   Response: Thank you for this helpful suggestion. To reflect this suggestion, in Introduction, we added a short discussion of how wake mixing can be implemented, supported by representative examples from the literature, as follows.

   Change in manuscript:

   Wake mixing enhances turbulent diffusion by promoting the entrainment of high-energy ambient flow into the wake, thereby accelerating wake recovery and improving inflow conditions for downstream turbines (van den Berg et al., 2024). Wake mixing can be implemented through blade pitch actuation and is categorized into Pulse method (collective pitch modulation) and Helix method (individual pitch modulation); a comparison of the resulting wake structures for both methods is provided in Fig. 2 in van den Berg et al. (2024).

3. **Comment:** *Line 59: a reference is needed to support the statement that the methods are cooperative rather than competitive.*

   Response and Change in manuscript: Thank you for this comment. We agree that our original wording could be interpreted as a general, literature-established claim. Our intent was to motivate the proposed framework, in which these strategies are treated as a set of candidate control actions whose combined effect is evaluated through the wake model and coordinated via numerical optimization. To avoid confusion, we removed the unsupported general statement.

4. **Comment:** *Line 59: it would be good to clarify that wake mixing is not combined with wake steering in the cited work.*

   Response: Thank you for this helpful comment. We added the following sentence in Introduction for the clarification.

   Change in manuscript:

   Note that, in the wake-mixing studies (Goit and Meyers, 2015; van den Berg et al., 2024; [6, 7, 8]), wake mixing was not applied simultaneously with other strategies.

5. **Comment:** *Line 109: the controller assumes knowledge of hub-height wind speed. Since this is difficult to measure in practice, adding a brief discussion would strengthen the paper.*

   Response: Thank you for this important comment. We added a brief discussion after equation (1) as follows.

   Change in manuscript:

   In the implementation of the controller, the free-stream wind speed at the hub height which is difficult to measure in practice is replaced by the rotor-effective wind speed estimate of the most upstream turbine. This estimate can be obtained from standard turbine measurements or via lidar-assisted methods [10, 11, 12, 13, 14, 15].

6. **Comment:** *Line 126: "Notably, power maximization can be regarded as a special case of power regulation by setting P_{ref} to the rated farm output", this sentence could be misleading, since the rated farm output typically refers to the greedy case, not to the power boosting case.*

Response: Thank you for this comment. We agree that the original wording "rated farm output" was misleading. To avoid this misunderstanding, we removed the sentence and added the following sentence to Section 3.2.1.

Change in manuscript:

For power maximization, the wind farm's reference power P_{ref} can be set to a sufficiently high (possibly unattainable) upper-bound target, such as the sum of rated turbine powers.

7. **Comment:** *Section 3: This section includes many repetitions of things that have been said already. It should be shortened in my opinion. For example:*

   - *Line 142: "A central challenge in wind farm operation is the presence of wake effects": this has been already said.*
   - *Lines 143–146, 161–163, 176–177, 184–186: These points appear to have been stated previously.*

   Response: Thank you for this helpful comment. In the revised manuscript, we streamlined Section 3 by removing or condensing the repeated explanations as follows.

   Change in manuscript:

   - **Lines 142-146 were condensed as follows:**
     Wake interactions reduce downstream power production and increase fatigue-relevant loading (see Fig. 3(a)), motivating coordinated wind farm control. In this work, we manipulate a set of available turbine-level inputs to mitigate wake overlap and improve farm-level performance.
   - **Lines 161–163 were shortened as follows:**
     Despite its potential, the repositioning capability of each turbine in a farm may be limited depending on wind conditions.
   - **Lines 176-177 were retained as they motivate the integrated framework, but were rephrased to avoid verbatim repetition:**
     This directional dependence motivates augmenting repositioning with additional strategies, including wake steering, power derating, and dynamic wake mixing.
   - **Lines 184–186 were shortened as follows:**
     Power derating constrains turbines to prescribed power caps P_{set}, thereby reducing wake deficits and alleviating downstream impacts (Fig. 3(d)).

8. **Comment:** *Line 150: it is not clear what β is. In line 188, there is a brief mention that this is the blade pitch angle. This is then the Helix approach, but there is no mention, description, or reference to it.*

   Response: Thank you for pointing this out. We agree that $\beta_{\text{amp},i}$ and the wake-mixing implementation were not introduced clearly. In response, we revised the manuscript as follows.

   Change in manuscript:

   - **Around Line 150:** We revised the definition to read:
     where θ_i (deg) is ..., and $\beta_{\text{amp},i}$ (deg) is the mean-to-peak amplitude of the sinusoidal blade-pitch excitation used for Helix wake mixing at turbine i ($i = 1, \ldots, N$).

- **Around Line 188:** We revised the description to read:
  In this study, wake mixing is realized using FLORIS's Helix mode (periodic individual blade-pitch actuation), with the wake-mixing intensity parameterized by the mean-to-peak excitation amplitude β_{amp} (van den Berg et al., 2024, [6, 7, 8]).

9. **Comment:** *Line 181: reference missing: "Although less effective than repositioning (CIT) ... "*

   Response: Thank you for this comment. We found this qualitative comparison was not essential to the paper and, without a clear supporting citation, could be misleading. We have therefore removed the sentence to avoid an unsupported comparative claim.

   Change in manuscript: We removed the sentence.

10. **Comment:** *Line 191: it seems like the authors are combining wake mixing with wake steering. This seems to push the capabilities of FLORIS a bit beyond its limits. As far as I know, there has not been any validation of this combination yet, and the effects do not really add up.*

    Response: Thank you for this important comment. Please see our response to General Comment 3.

11. **Comment:** *Line 209: introducing weights in the cost function is sometimes inevitable, but it introduces important choices. How were these weights set and why? Was the cost function normalized somehow? The power tracking error and the velocity error have substantial differences in order of magnitude.*

    Response: Thank you for this important comment. In response, to reduce redundancy, we revised the cost function (5) by dropping the power tracking weight. Consequently, only the wake mitigation term remains to be selected. This weight was tuned via trial and error to obtain an acceptable trade-off. We did not apply a normalization. The manuscript has been revised accordingly, as shown below.

    Change in manuscript:

    The cost function (5) is revised to:

    $$J(\mathbf{U}) = (P_{\text{ref}} - \sum_{i=1}^{N} P_i)^2 + w \sum_{i=1}^{N} \|\underline{v}_\infty - \underline{v}_i\|^2. \tag{5}$$

    We also added a short discussion on the weight selection:

    The power-tracking term and the wake-mitigation term in (5) have different units and typical magnitudes; therefore, the constant weight w is a key design parameter. It is to be selected via trial and error to balance the relative influence of the two terms.

12. **Comment:** *Section 3.2.1: More detail is needed on how turbines are curtailed. The method strongly affects the thrust coefficient, so describing the approach is important.*

    Response: Thank you for this important comment. We revised Section 3.2.2 to describe how power derating is implemented in FLORIS as follows.

    Changes in manuscript:

Power derating is implemented by prescribing a per-turbine power cap $P_{\text{set},i}$. This setpoint is passed to FLORIS's "simple-derating" turbine operation model, which first evaluates the turbine power P_i and thrust coefficient from the power-thrust table at the local inflow and then enforces the cap as $P_i = \min\{P_i, P_{\text{set},i}\}$. When the cap limits the power output, FLORIS reduces the turbine thrust coefficient accordingly to reflect the curtailed operating point.

13. **Comment:** *Line 242: since a genetic algorithm is used with a large number of scenarios and variables, a short note on convergence criteria or computational considerations would be insightful.*

    Response:

    Thank you for this helpful suggestion. We agree that reporting the termination criteria and computational cost improves the transparency and reproducibility of the results. We have therefore added a short note in Section 4.1 summarizing the genetic algorithm settings, and representative runtime.

    Change in manuscript:

    For the numerical studies in this work, we solve (4) using a standard genetic algorithm as implemented in pymoo [16]. The single-objective genetic algorithm was run with a population size of 80 and a maximum of 80 generations. For the considered case studies, the wall-clock time per optimization run was on the order of 15 minutes on a Windows 11 workstation with an Intel Core i9-13900HX CPU (24 cores/32 threads) and 32 GB RAM.

14. **Comment:** *Line 262: how was power maximization achieved with the cost function in Eq. (5)? This seems to apply only to power regulation.*

    Response: Thank you for this comment. We agree that Eq. (5) may look like a power regulation/tracking objective at first glance. In our framework, "power maximization" is implemented through the same tracking form by setting the reference P_{ref} to a sufficiently high (possibly unattainable) upper-bound target, such as the sum of rated turbine powers. We have modified the manuscript in Section 3.2.1 to clarify this point as follows.

    Change in manuscript:

    For power maximization, the wind farm's reference power P_{ref} can be set to a sufficiently high (possibly unattainable) upper-bound target, such as the sum of rated turbine powers.

15. **Comment:** *Line 265: was a wind rose considered here? What turbulence intensity was set?*

    Response: Thank you for this comment. We have clarified this in Section 4.2.1 as follows.

    Change in manuscript:

    Fig. 7 shows the maximum achievable farm power for steady inflow wind speeds of 4, 6, 8, and 10 m/s as the inflow direction is swept over the full 0-360 degrees range (without wind-rose probability weighting). Wind direction is defined clockwise from the top of the wind farm (0 degrees at the top). All simulations assume an ambient turbulence intensity of 0.06, a power-law vertical shear exponent of 0.12, and zero wind veer.

16. **Comment:** *Figure 9: showing local inflow velocities would be informative, since they also appear in the cost function.*

Response: Thank you for this helpful suggestion. In the revised manuscript, rather than showing local inflow velocities in Fig. 8 (original Fig. 9), we annotated the local turbine inflow velocities in Figs. 9-10 (panels (a), (b), (d), and (e)), as this provides a more direct visualization of the velocity quantities used in the cost function. These panels correspond to original Figs. 10-13.

Change in manuscript: See Figs. 9-10 (panels (a), (b), (d), and (e)).

17. **Comment:** *Figure 9: the histograms refer to wake mixing, wake steering and integrated control. It would be interesting to see also the effect of repositioning alone.*

    Response: Thank you for this comment. In response, we added results for repositioning together with wake steering in Figs. 7-8 (original Fig. 8-9). Note that "repositioning alone" is not possible; repositioning of floating offshore wind turbines via aerodynamic thrust force is incurred by net yaw angle which steers the wake.

    Changes in manuscript: See Figs. 7-8.

18. **Comment:** *Line 306: the power regulation case was run at a wind speed of 18 m/s. Since this is above rated for most turbines, the controller behavior may be less interesting there. Running it in region II might give more insight. A brief explanation of the choice would help.*

    Response: Thank you for this helpful comment. We agree that presenting a region II power-regulation case can provide more insight into the controller behavior. In response, we revised the Results section to report the power-regulation case at 10 m/s instead of 18 m/s.

    Change in manuscript: See Fig. 10.

19. **Comment:** *Line 340: I encourage the authors to consider open-access sharing platforms, as this greatly supports reproducibility.*

    Response: Thank you for this helpful suggestion. In response, we have publicly shared the code and revised the Data and Code Availability statement as follows.

    Change in manuscript:

    The code used in this study is publicly available at `https://drive.google.com/drive/folders/1h6ebwumd06PdEuX38KJgqEwQK9Lhss3e`.

20. **Technical comments**

    (a) **Comment:** *Line 126: reference missing: "... or ancillary service needs (CIT)"*
    Response and Change in manuscript: Thank you for this comment. We added a reference [17].

    (b) **Comments on figures:**

    - *Figure 8 is difficult to read in black/white.*
    - *Figures 10a, 10b, 11a, 11b, 12a, 12b, 13a, 13b: axis labels should be added.*
    - *In figures 10c, 11c, 12c, 13c, it is not entirely clear what the histograms represent; a short explanation in the caption would help.*

    Response: Thank you for this comment. We revised the figures to improve readability as follows.

    Change in manuscript:

- Figure 7 (original Figure 8): We introduced different line styles and markers.
- Figures 9 and 10 (original Figures 10-13): We added axis labels.
- Figures 9 and 10 (original Figures 10c-13c): We revised captions to state what the histograms represent.

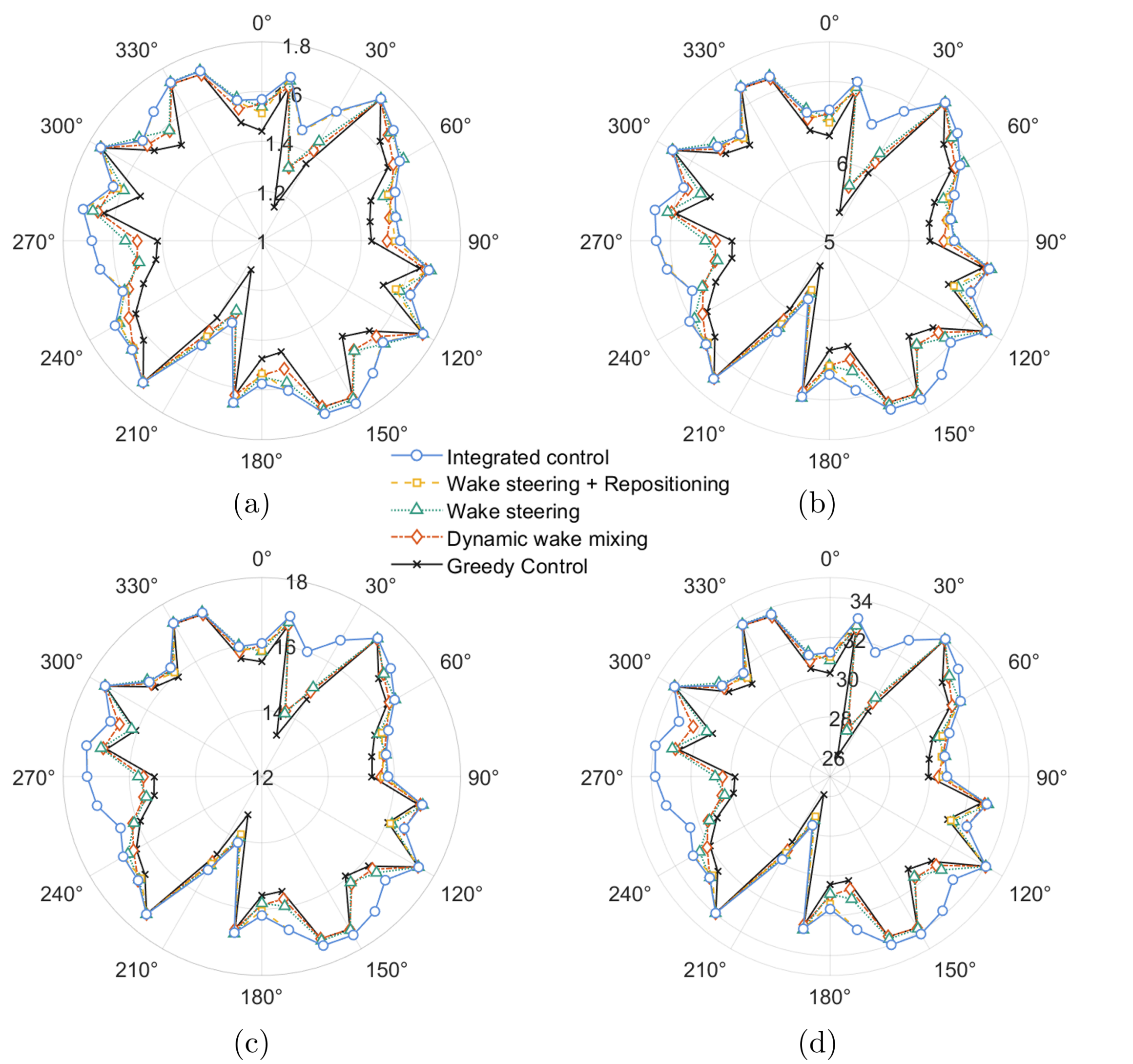

Figure 7: Maximum achievable farm power as a function of inflow wind direction for four steady wind speeds: (a) 4 m/s, (b) 6 m/s, (c) 8 m/s, and (d) 10 m/s. Each polar plot compares the optimized farm power (MW; numbers annotated inside the plots) obtained under integrated control (turbine repositioning + wake steering + dynamic wake mixing), wake steering + repositioning, wake steering only, dynamic wake mixing only, and greedy control. Direction-dependent "notches" indicate inflow directions with severe wake effects and associated power deficits under greedy operation. Across wind speeds, the integrated controller consistently mitigates wake effects and provides the highest power envelope over direction, illustrating the benefit of coordinated control mechanisms.

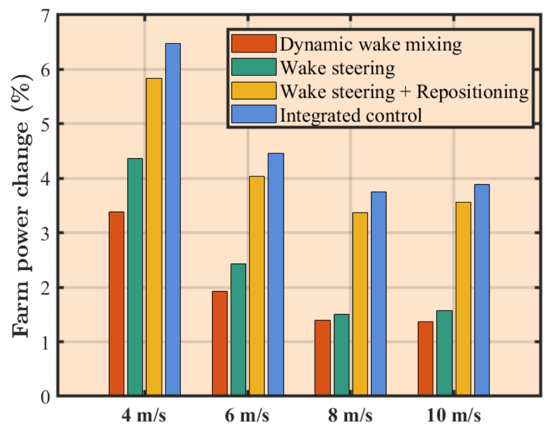

Figure 8: Average improvement in maximum farm power over the full 0-360 degrees inflow-direction sweep for wind speeds of 4-10 m/s, expressed as percent change relative to greedy control. Bars compare integrated control, wake steering + repositioning, wake steering, and dynamic wake mixing, highlighting the consistent benefit of integrated strategies.

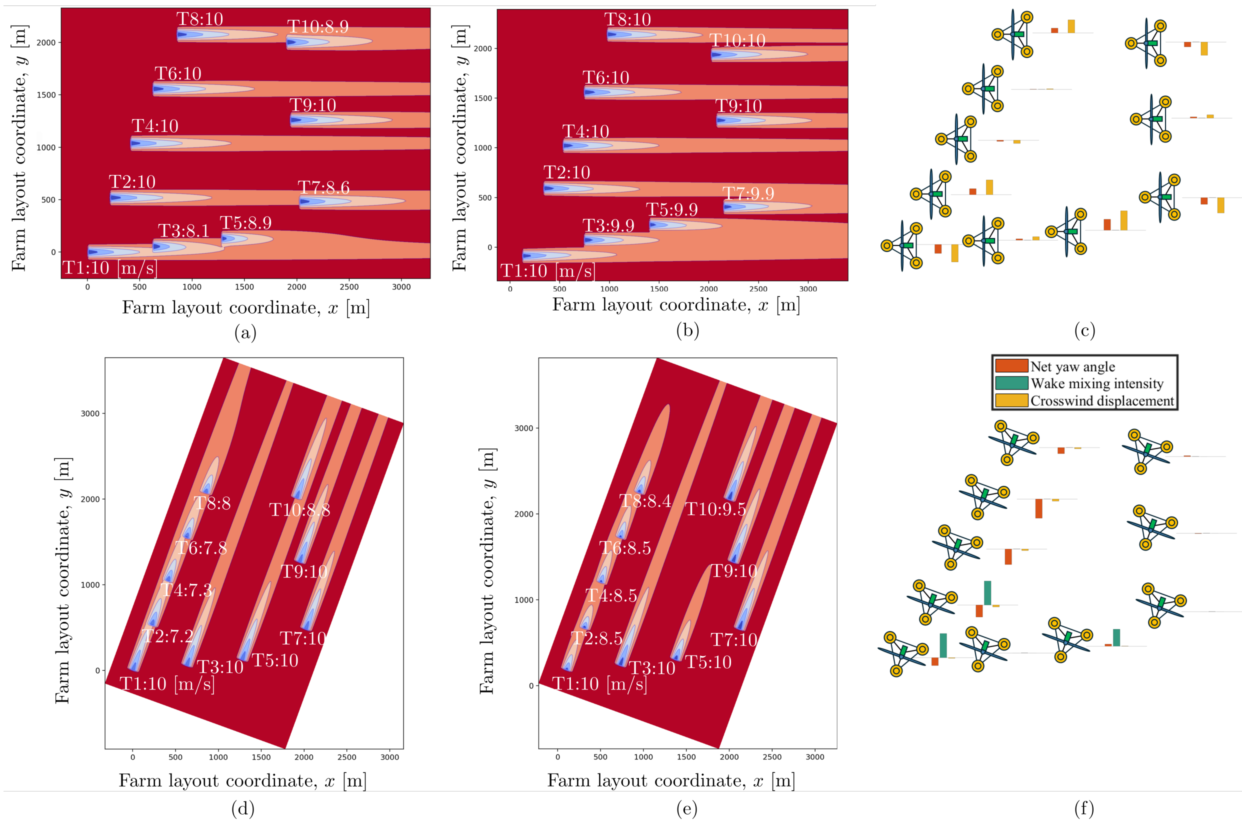

Figure 9: Representative power-maximization results at an inflow speed of 10 m/s for two inflow directions. Panels (a)-(c) correspond to wind from the left, and panels (d)-(f) correspond to wind from the lower-left. For each case, panels (a) and (d) show the hub-height wind-speed field under greedy control, and panels (b) and (e) show the corresponding field under integrated control. Color denotes wind speed (red: near free-stream; white/blue: wake deficits), and the numbers annotated near each turbine indicate the corresponding local turbine inflow velocity. Panels (c) and (f) summarize the integrated control solution with per-turbine bar plots of net yaw angle, Helix excitation amplitude, and crosswind displacement. These quantities are normalized by 20 degrees, 5 degrees, and 120 m, respectively; bars close to zero indicate negligible use, whereas larger magnitudes indicate greater control effort, and bars above/below zero indicate opposite yaw/displacement directions. With substantial crosswind mobility in the left-inflow case, the controller primarily exploits repositioning to reduce wake overlap and maximize farm power. With limited crosswind mobility in the lower-left inflow case, the controller relies on wake steering and Helix wake mixing to mitigate wake effects.

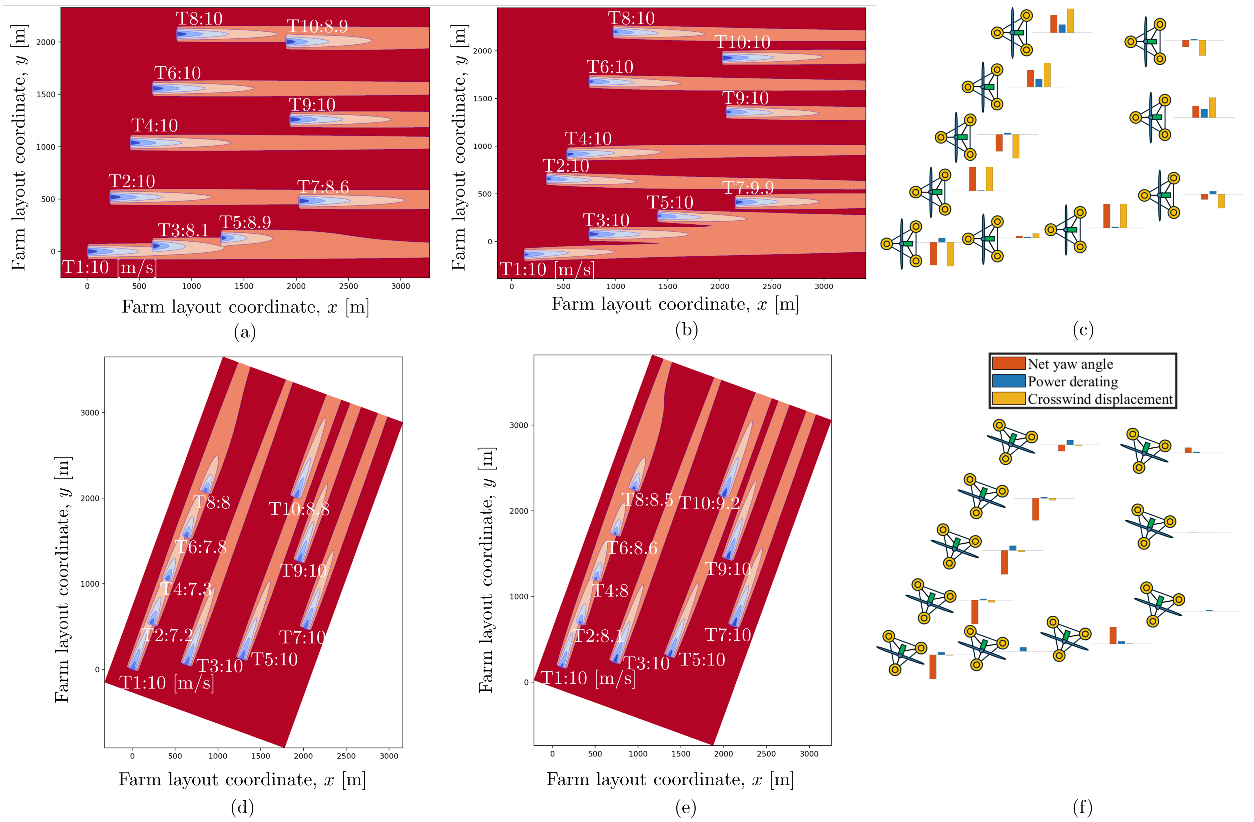

Figure 10: Representative power-regulation results at an inflow speed of 10 m/s for two inflow directions. Panels (a)-(c) correspond to wind from the left with $P_{\mathrm{ref}} = 32$ MW, and panels (d)-(f) correspond to wind from the lower-left with $P_{\mathrm{ref}} = 27$ MW. For each case, panels (a) and (d) show the hub-height wind-speed field under greedy control, and panels (b) and (e) show the corresponding field under integrated control. Color denotes wind speed (red: near free-stream; white/blue: wake deficits), and the numbers annotated near each turbine indicate the corresponding local turbine inflow velocity. Panels (c) and (f) summarize the integrated control solution with per-turbine bar plots of net yaw angle, derating level $(5\ \mathrm{MW} - P_{\mathrm{set},i})/5$ MW, and crosswind displacement. In the left-inflow case, the controller leverages the available crosswind mobility to reposition turbines and alleviate wake overlap, while using distributed derating and associated yaw-induced power reduction to satisfy the farm-level power reference. With limited crosswind mobility in the lower-left inflow case, the controller relies on wake steering, together with distributed derating, to reduce wake overlap while tracking the farm-level power reference.

Responses to Reviewer 2

General comments

1. **Comment:** *The methodology needs to be expanded to specify in more detail all the elements that are included in the proposed framework. In particular, it remains unclear which dynamic wake mixing method is used. In addition, as also noted by the other reviewer, the paper heavily relies on FLORIS. While FLORIS is fundamentally a steady-state engineering model, it could indeed be possible that some dynamic effects (e.g., dynamic wake mixing) are approximated, simulated, or evaluated within your setup. If so, this requires a detailed justification in the methodology section.*

   Response: Thank you for this important comment. We agree that the original manuscript did not describe the framework components and the wake-mixing model with sufficient clarity. We have expanded the methodology to provide a more complete description of the proposed framework; the corresponding revisions are reflected throughout our responses to the remaining comments. Since this comment specifically concerns wake mixing, we summarize below the key clarifications and manuscript changes related to the (Helix) wake-mixing method as follows.

   Change in manuscript:

   - **Abstract:** revised to explicitly list the coordinated control methods:
     The framework coordinates four farm-level control strategies, that is, turbine repositioning, wake steering, power derating, and Helix wake mixing, to either (i) maximize total farm power output or (ii) track a prescribed farm-level power setpoint while mitigating wake effects.
   - **Introduction:** added sentences defining terminology and scope:
     In this paper, "dynamic wake mixing" refers to Helix wake mixing realized via periodic individual-blade pitch excitation.
     This study focuses on steady-state (time-averaged) farm-level aerodynamic performance; transient wake dynamics are beyond the scope of the present FLORIS-based evaluation.
   - **Section 3.1:** revised to define the wake-mixing parameter clearly:
     where θ_i (deg) is ..., and $\beta_{\mathrm{amp},i}$ (deg) is the mean-to-peak amplitude of the sinusoidal blade-pitch excitation used for Helix wake mixing at turbine i ($i = 1, \ldots, N$).
   - **Section 3.1.2:** clarified the Helix-mode implementation and parametrization:
     In this study, wake mixing is realized using FLORIS's Helix mode (periodic individual blade-pitch actuation), with the wake-mixing intensity parameterized by the mean-to-peak excitation amplitude β_{amp} (van den Berg et al., 2024, [6, 7, 8]).
   - **Section 3.2.2:** added a clarification of the wake-mixing implementation:
     Helix wake mixing is represented using FLORIS's built-in active wake control "helix" operation model, which parameterizes the time-averaged impact of helix pitch excitation on turbine power/thrust and wake recovery and has been calibrated in FLORIS as a standalone wake-mixing representation.
   - **Section 4.1:** added a clarification of the selected maximum mean-to-peak amplitude:

The Helix excitation amplitude is bounded to $\beta_{\text{amp},i} \in [0, 5]$ degrees, where $\beta_{\text{amp},i} = 0$ corresponds to no wake-mixing actuation and the upper bound is consistent with excitation levels reported in prior studies (e.g., up to 4 degrees in van den Berg et al., 2024, and up to 5 degrees in [6]).

2. **Comment:** *I also miss a discussion on the presumed constant yaw angle that is required when relocating a turbine from its initial position, and the possible steady and periodic structural loads this introduces. Furthermore, you assume a hub-height wind speed measurement; would a rotor-effective wind speed (REWS) not be a better representation, especially given increasing turbine sizes?*

   Response: Thank you for this important comment. We agree that (i) sustaining a yaw misalignment for repositioning can introduce additional mean and fatigue-relevant cyclic loads, and (ii) assuming direct access to the free-stream hub-height wind speed is idealized. We have revised the manuscript to address both points as follows.

   Change in manuscript:

   - **Introduction:** added the following statement:

     Notably, a nonzero yaw offset is required to be sustained to balance mooring restoring forces at the repositioned position. Sustained yaw offsets can alter both mean and cyclic component loads (e.g., blade-root bending moments and tower loads) and thus influence fatigue [18]; quantifying these fatigue implications is beyond the scope of the present study.

   - **Section 4.1:** added the following clarification:

     The proposed coordination framework is evaluated in FLORIS for farm-level aerodynamic performance and does not explicitly quantify structural load or fatigue impacts of sustained yaw misalignment. To avoid excess fatigue loads, the net yaw offset is constrained to $|\theta| \leq 20$ degrees; a coupled aeroelastic analysis (e.g., OpenFAST/FAST.Farm) is required in future work to assess the associated loading and fatigue implications.

   - **After Eq. (1):** revised the manuscript to include a brief discussion and to cite relevant literature:

     In the implementation of the controller, the free-stream wind speed at the hub height which is difficult to measure in practice is replaced by the rotor-effective wind speed estimate of the most upstream turbine. This estimate can be obtained from standard turbine measurements or via lidar-assisted methods [10, 11, 12, 13, 14, 15].

3. **Comment:** *I also do not understand the choice for the multi-objective NSGA-II optimizer; you appear to have a single objective.*

   Response: Thank you for this thoughtful comment. You are absolutely right—our formulation uses a single objective (a weighted-sum cost), and thus a multi-objective optimizer is unnecessary. Following your suggestion, we removed NSGA-II from the manuscript and now state the solver choice more appropriately: we describe the problem in general as requiring a global optimization approach, and we specify that a standard genetic algorithm (GA) solver is used in this study as follows. In addition, we re-ran the simulations using the GA-based implementation, and all reported results in the revised manuscript are generated with this updated solver.

Change in manuscript:

- **In Section 3.2.4, the sentence describing NSGA-II was revised to:**
  Overall, the optimization problem formulated in (4) is nonlinear and nonconvex because of ..., which can be solved using a global optimization solver.
- **In Section 4.1, we clarified the solver used in the numerical studies as:**
  For the numerical studies in this work, we solve (4) using a standard genetic algorithm as implemented in pymoo [16].

4. **Comment:** *I like the high-quality, self-created figures, but please include more elaborate captions underneath them, explaining what can be seen and what can be concluded.*

   Throughout the paper: include more elaborate figure captions. Clearly state what is shown, what the remarkable elements are, and what conclusions can be drawn.

   Response: Thank you for this encouraging feedback and helpful suggestion. We revised the captions throughout the manuscript to be more informative and self-contained. In particular, we expanded each caption to briefly (i) describe what is plotted and the key visual elements (e.g., color meaning, scenarios/inputs, and compared control strategies), and (ii) state the main takeaway that the figure supports (e.g., performance improvements, dominant strategy selection under constrained mobility, or improved wake recovery/overlap reduction).

   Change in manuscript: See Figs. 5 and 7-10 included in this file, and refer to the revised manuscript for the remaining figures.

5. **Comment:** *the methodology in particular needs to be expanded, with stronger justification of the modeling and optimization choices that were made. I therefore suggest a major revision.*

   Response: Thank you for this important comment. We agree that the original manuscript did not provide sufficient methodological detail and justification for modeling and optimization choices. In response, we undertook major revisions to improve transparency, reproducibility, and interpretation of the results. The main revisions are summarized below.

   Change in manuscript:

   - **Section 3.2.2:** added an explicit description of the FLORIS wake-modeling choices:
     In this study, wake effects in FLORIS are represented by four submodels, each used with the default parameter values provided by FLORIS [1]:
     - **Velocity deficit model:** For the wake velocity deficit, we use the empirical Gaussian wake model, which assumes a Gaussian distribution of the velocity deficit [2, 3].
     - **Wake deflection model:** Wake deflection is computed using FLORIS's empirical Gaussian deflection model based on yaw-misalignment wake-deflection formulations [2, 3].
     - **Wake turbulence model:** To account for added turbulence in turbine wakes, we employ the wake-induced mixing model in FLORIS, which generalizes wake-added turbulence in the empirical Gaussian wake model [4]. In this model, upstream turbines contribute to mixing in the flow, yielding a wake-induced mixing factor

that is passed to the velocity deficit and wake deflection models to modify the wake width and the wake-centerline deflection, respectively.

  - **Wake combination model:** Wake effects from multiple turbines are combined using the sum-of-squares freestream superposition model [5].

- Clearly specified the implementation of Helix wake mixing in FLORIS (see our response to General Comment 1),

- **Section 3.2.2:** clarified how power derating and Helix wake mixing are implemented in FLORIS, and explicitly stated the assumptions/limitations associated with their combined application with yaw misalignment:

  The wind farm control methods are implemented in FLORIS through the control inputs $\mathbf{U}$ as follows:

  - **Wake steering:** Wake steering is implemented by prescribing yaw misalignment commands θ_i, which modify turbine power/thrust and the resulting wake deflection in a steady-state sense.
  - **Turbine repositioning:** Turbine repositioning is represented by the same yaw commands θ_i but is coupled with a steady-state turbine position solver (see Sect. 3.2.4) that enforces static equilibrium between aerodynamic loading and mooring restoring forces to update the turbine positions. The updated positions are then evaluated in FLORIS, thereby changing wake overlap and farm performance.
  - **Power derating:** Power derating is implemented by prescribing a per-turbine power cap $P_{\text{set},i}$. This setpoint is passed to FLORIS's "simple-derating" turbine operation model, which first evaluates the turbine power P_i and thrust coefficient from the power-thrust table at the local inflow and then enforces the cap as $P_i = \min\{P_i, P_{\text{set},i}\}$. When the cap limits the power output, FLORIS reduces the turbine thrust coefficient accordingly to reflect the curtailed operating point.
  - **Helix wake mixing:** Helix wake mixing is represented using FLORIS's built-in active wake control "helix" operation model, which parameterizes the time-averaged impact of helix pitch excitation on turbine power/thrust and wake recovery and has been calibrated in FLORIS as a standalone wake-mixing representation.

  It should be noted that FLORIS has not yet been extensively validated for cases in which a turbine is simultaneously yaw-misaligned and operated in either derated mode or active wake-mixing mode. In our optimization framework, we nevertheless allow yaw misalignment to be applied concurrently with either power derating or Helix wake mixing for each turbine. Under such combined operation, FLORIS predicts steady-state changes in turbine power/thrust, wake deflection, and wake recovery; however, the corresponding results should be interpreted with this validation limitation in mind. Moreover, when wake steering and power derating/Helix wake mixing are applied simultaneously, yaw-induced power loss is not captured (as observed in our simulations) in the FLORIS prediction; therefore, to avoid overestimating power capture under yaw misalignment, we apply a yaw-power loss correction for yawed turbines, $P_i \leftarrow P_i(\cos\theta_i)^{p_P}$, with a parameter value $p_P = 1.88$ [9]. For yaw-only wake-steering/turbine-repositioning cases, we do not apply this additional correction to avoid double counting.

- **Section 4.1:** following the reviewer's suggestion, we removed NSGA-II and instead used a standard single-objective genetic algorithm (GA), which is more appropriate for the weighted-sum objective considered here. We re-ran all simulations using the GA-based implementation, and the revised manuscript now reports the solver settings, termination criteria, and representative computational cost (see our response to General Comment 3 and the added text below):

The single-objective genetic algorithm was run with a population size of 80 and a maximum of 80 generations. For the considered case studies, the wall-clock time per optimization run was on the order of 15 minutes on a Windows 11 workstation with an Intel Core i9-13900HX CPU (24 cores/32 threads) and 32 GB RAM.

- **Section 4.2.1:** added the ambient inflow conditions:

  All simulations assume an ambient turbulence intensity of 0.06, a power-law vertical shear exponent of 0.12, and zero wind veer.

Specific comments

1. **Abstract and Introduction**

   (a) **Comment:** What does "regulate it to a prescribed reference" mean? Does this refer to total farm power?

   Response: Thank you for this comment. Yes. By "regulate it to a prescribed reference," we mean regulating the total wind-farm power output to track a commanded farm-level setpoint. We have revised the abstract to make this meaning explicit as follows.

   Change in manuscript:

   The framework coordinates four farm-level control strategies, that is, turbine repositioning, wake steering, power derating, and Helix wake mixing, to either (i) maximize total farm power output or (ii) track a prescribed farm-level power setpoint while mitigating wake effects.

   (b) **Comment:** *I also find the description of the integrated/unified framework unclear. Only at the end of the introduction does it become apparent that this is an optimization framework. After reading the first sentences of the abstract, it is not clear what the work entails. These sentences form the core of the abstract but currently lack clarity.*

   Response: Thank you very much for this helpful comment. In response, we revised the opening sentences of the abstract to improve clarity as follows.

   Change in manuscript:

   This paper proposes an integrated optimization-based control framework for floating offshore wind farms (FOWFs) with reconfigurable layouts. The framework coordinates four farm-level control strategies, that is, turbine repositioning, wake steering, power derating, and Helix wake mixing, to either (i) maximize total farm power output or (ii) track a prescribed farm-level power setpoint while mitigating wake effects.

   (c) **Comment:** *What is the input to your framework (reference/setpoint/demand), and what are its outputs? Please make this explicit.*

   Response: Thank you for this comment. We have revised the abstract to explicitly state the framework's inputs and its outputs as follows.

   Change in manuscript:

   Given the ambient inflow conditions (wind speed and direction), the framework computes coordinated per-turbine commands, including yaw angles, derating commands that limit each turbine's power to not exceed a prescribed value, and mean-to-peak amplitude of sinusoidal blade-pitch excitation, to meet the farm power requirement and to reduce the wake overlap.

(d) **Comment:** *If a turbine is relocated from its initial position via yaw misalignment, this yaw misalignment must be maintained to compensate for the restoring force of the mooring lines. I believe the introduction should already mention the additional rotor and structural loads (both steady and periodic) that this induces.*

Response: Thank you for this important comment. We agree. In response, we added a brief statement in the Introduction. Please see our response to General Comment 2.

(e) **Comment:** *It remains unclear in both the abstract and introduction what type of "dynamic wake mixing" is intended. Is this dynamic induction using a sinusoidal, helical, or other approach? This should be clarified early in the paper.*

Response: Thank you for this important comment. We have clarified this explicitly in both the abstract and the introduction. Please see our response to General Comment 1.

2. **Section 2**

(a) **Comment:** *You assume access to the free-stream wind speed at hub height. Would it not be more appropriate to use a rotor-effective wind speed estimate (REWS) rather than a single hub-height measurement? You could potentially alleviate this assumption by estimating wind speed using a REWS estimator. Please comment on this and consider referencing relevant literature.*

Response: Thank you for this important comment. We agree that, in practice, using a rotor-effective wind speed estimate is more appropriate than assuming direct access to the free-stream hub-height wind speed. In response, we revised the manuscript to include a brief discussion and to cite relevant literature after equation (1), as follows.

Change in manuscript:

In the implementation of the controller, the free-stream wind speed at the hub height which is difficult to measure in practice is replaced by the rotor-effective wind speed estimate of the most upstream turbine. This estimate can be obtained from standard turbine measurements or via lidar-assisted methods [10, 11, 12, 13, 14, 15].

(b) **Comment:** *Consider renaming "power regulation" to "power derating" throughout the paper.*

Response: Thank you for this comment, and we apologize for any confusion. In this paper, *power regulation* refers to the farm-level control objective of tracking a prescribed farm power reference, whereas *power derating* is one of the control strategies used to achieve that objective by intentionally limiting selected turbine power outputs. Power regulation may also be achieved through other strategies such as wake steering, which can reduce turbine power by introducing intentional yaw misalignment. To avoid confusion, we revised Section 3.1 as follows.

Change in manuscript:

To avoid confusion, we distinguish turbine-level derating, implemented via $P_{\text{set},i}$, from farm-level power regulation, which refers to tracking a prescribed farm power reference P_{ref} through coordinated turbine commands.

3. **Section 3**

   (a) **Comment:** *"$\beta_{amp,i}$ (deg), the wake mixing intensity of turbine i": what exactly does this represent? Is this related to dynamic induction control, where β_{amp} is the amplitude of a sinusoidal yaw signal, or to a helical implementation? Please clarify.*

   Response: Thank you for pointing this out. We agree that $\beta_{\text{amp},i}$ and the wake-mixing implementation were not introduced clearly. In response, we revised the manuscript as follows.

   Change in manuscript:

   - **Around Line 150:** We revised the definition to read:
     where θ_i (deg) is ..., and $\beta_{\text{amp},i}$ (deg) is the mean-to-peak amplitude of the sinusoidal blade-pitch excitation used for Helix wake mixing at turbine i ($i = 1, \ldots, N$).
   - **Around Line 188:** We revised the description to read:
     In this study, wake mixing is realized using FLORIS's Helix mode (periodic individual blade-pitch actuation), with the wake-mixing intensity parameterized by the mean-to-peak excitation amplitude β_{amp} (van den Berg et al., 2024, [6, 7, 8]).

   (b) **Comment:** *"The wind comes from the right, representing the worst case with a relative angle of 60 degrees." Left or right? Please double-check, and also clarify the 60-degree relative angle.*

   Response: Thank you for this comment, and we apologize for the confusion. To remove ambiguity, we eliminated the "relative angle" description and revised both the figure caption and the associated discussion as follows.

   Change in manuscript:

   Despite its potential, the repositioning capability of each turbine in a farm may be limited depending on wind conditions. For the symmetric three-line mooring system in Fig. 5(a), assume that the wind blows from left to right and the net yaw angle is set to $\theta = 0$. The turbine drifts downwind to an equilibrium where the wind-aligned mooring line becomes load-bearing and the other two lines slacken; consequently, crosswind motion encounters relatively little resistance and substantial repositioning becomes possible. By contrast, when the wind blows from right to left (Fig. 5(b)), the two right-side mooring lines remain taut and jointly oppose the motion, which increases restoring stiffness and severely restricts lateral displacement, reducing the effectiveness of repositioning. This directional dependence motivates augmenting repositioning with additional strategies, including wake steering, power derating, and dynamic wake mixing.

   (c) **Comment:** *Again, how are the structural loads associated with such large turbine–wind misalignments accounted for or justified?*

   Response: Thank you for this important comment. We agree that sustained yaw misalignment can affect both mean and fatigue-relevant cyclic structural loads, and that these load effects are not captured in the present FLORIS-based study. To avoid excess fatigue loads, we impose an operational constraint on the net yaw misalignment, $|\theta| \leq 20$ degrees. Please see our response to General Comment 2.

   (d) **Comment:** *Fig. 6: I do not understand the last subfigure, where you state that there is a 60-degree relative angle. The turbine appears rotated by 180 degrees, and the wind now comes from the right. What is the difference compared to the second subfigure?*

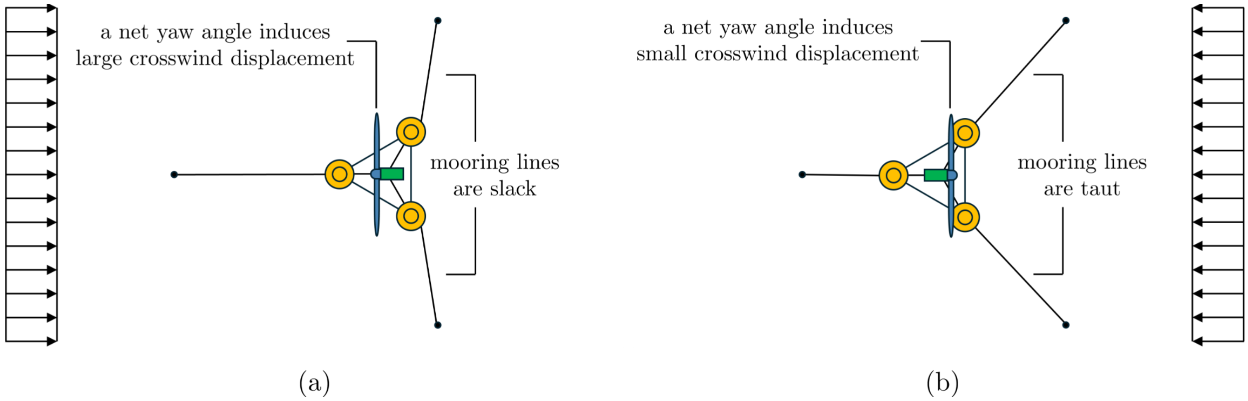

Figure 5: Illustration of a limitation of turbine repositioning. (a) Wind from left to right: one mooring line is primarily load-bearing while the other two slacken, allowing relatively unconstrained crosswind motion. (b) Wind from right to left: two mooring lines remain taut and oppose the motion, limiting crosswind displacement.

Response and Change in manuscript: Thank you for this comment, and we apologize for the confusion. We address this point in our response to Comment 3(b) above.

(e) **Comment:** *Eq. (5): You could omit one of the weights (e.g., normalize one to unity) and only optimize the other, which would simplify the definition of the objective function.*

Response: Thank you for this helpful suggestion. We followed this advice by dropping the power tracking weight. The manuscript has been revised as follows.

Change in manuscript:

The objective function (5) is revised to:

$$J(\mathbf{U}) = (P_{\text{ref}} - \sum_{i=1}^{N} P_i)^2 + w \sum_{i=1}^{N} \|\underline{v}_\infty - \underline{v}_i\|^2. \tag{5}$$

(f) **Comment:** *The choice of the NSGA-II algorithm is somewhat surprising. NSGA-II is designed for multi-objective optimization, and its core mechanisms are unnecessary or inefficient for a single-objective problem. Since you appear to have a single objective function, why not use a standard genetic algorithm (GA) or particle swarm optimization (PSO)?*

Response: Thank you for this thoughtful comment. We address this point in our response to General Comment 3 above.

4. **Section 4**

(a) **Comment:** *You repeatedly state that dynamic wake mixing is part of your framework. However, FLORIS is a steady-state, time-averaged engineering model and does not inherently simulate transient or dynamic wake evolution. Am I missing something here? How exactly is FLORIS used to evaluate the effects of dynamic wake mixing?*

Response: Thank you for this important comment. We understand that FLORIS is a steady-state, time-averaged engineering model and does not resolve transient wake evolution in the time domain. Accordingly, in this study, FLORIS is not used to simulate the instantaneous dynamics of wake mixing. Instead, the effect of wake mixing is evaluated using FLORIS's built-in active wake control operational model, specifically the "helix" mode, which parameterizes the time-averaged effects of helix pitch excitation on turbine power/thrust. To clarify this point, we added the sentences below.

Change in manuscript:

- **Introduction:** We added the following sentence:
  This study focuses on steady-state (time-averaged) farm-level aerodynamic performance; transient wake dynamics are beyond the scope of the present FLORIS-based evaluation.
- **Section 3.2.2:** We added the following sentence:
  Helix wake mixing is represented using FLORIS's built-in active wake control "helix" operation model, which parameterizes the time-averaged impact of helix pitch excitation on turbine power/thrust and wake recovery and has been calibrated in FLORIS as a standalone wake-mixing representation.

5. **Conclusion**

(a) **Comment:** *"Overall, these findings demonstrate that coordinating multiple control strategies, rather than applying them in isolation," — do you mean "multiple control objectives" instead of "control strategies"?*

Response: Thank you for this comment. We mean multiple control strategies (turbine repositioning, wake steering, power derating, and dynamic wake mixing), not multiple control objectives. In response, we revised the sentence to avoid confusion as follows.

Change in manuscript:

Overall, these findings demonstrate that coordinating multiple control strategies (turbine repositioning, wake steering, power derating, and dynamic wake mixing), rather ...

References

[1] National Renewable Energy Laboratory. "FLORIS version 4.4.2." GitHub. Accessed: Aug. 22, 2025. [Online]. Available: https://github.com/NREL/floris

[2] M. Bastankhah and F. Porté-Agel, "Experimental and theoretical study of wind turbine wakes in yawed conditions," *Journal of Fluid Mechanics*, vol. 806, pp. 506–541, 2016.

[3] J. King, P. Fleming, R. King, L. A. Martínez-Tossas, C. J. Bay, R. Mudafort, and E. Simley, "Control-oriented model for secondary effects of wake steering," *Wind Energy Science*, vol. 6, no. 3, pp. 701–714, 2021.

[4] National Renewable Energy Laboratory. "floris.core.wake_turbulence.wake_induced_mixing". Accessed: Jan. 05, 2026. [Online]. Available: https://nrel.github.io/floris/_autosummary/floris.core.wake_turbulence.wake_induced_mixing.html

[5] ——. "floris.core.wake_combination.sosfs". Accessed: Jan. 05, 2026. [Online]. Available: https://nrel.github.io/floris/_autosummary/floris.core.wake_combination.sosfs.html

[6] T. Dammann, D. van der Hoek, W. Yu, and J.-W. van Wingerden, "Enhanced wind farm performance via active wake control: A steady-state approach," in *2025 American Control Conference*, Denver, CO, USA, July 2025, pp. 2856–2861.

[7] A. A. W. van Vondelen, M. Coquelet, S. T. Navalkar, and J.-W. van Wingerden, "Synchronized helix wake mixing control," *Wind Energy Science*, vol. 10, no. 10, pp. 2411–2433, 2025.

[8] A. A. van Vondelen, D. C. van der Hoek, S. T. Navalkar, and J.-W. van Wingerden, "Experimental validation of synchronized helix wake mixing control," *Renewable Energy*, vol. 257, 2026, Art. no. 124768.

[9] P. M. O. Gebraad, F. W. Teeuwisse, J. W. van Wingerden, P. A. Fleming, S. D. Ruben, J. R. Marden, and L. Y. Pao, "Wind plant power optimization through yaw control using a parametric model for wake effects—a CFD simulation study," *Wind Energy*, vol. 19, no. 1, pp. 95–114, 2016.

[10] K. Z. Østergaard, P. Brath, and J. Stoustrup, "Estimation of effective wind speed," *Journal of Physics: Conference Series*, vol. 75, no. 1, July 2007, Art. no. 012082.

[11] M. N. Soltani, T. Knudsen, M. Svenstrup, R. Wisniewski, P. Brath, R. Ortega, and K. Johnson, "Estimation of rotor effective wind speed: A comparison," *IEEE Transactions on Control Systems Technology*, vol. 21, no. 4, pp. 1155–1167, 2013.

[12] D. P. Held and J. Mann, "Lidar estimation of rotor-effective wind speed – an experimental comparison," *Wind Energy Science*, vol. 4, no. 3, pp. 421–438, 2019.

[13] D. Schlipf, P. W. Cheng, and J. Mann, "Model of the correlation between lidar systems and wind turbines for lidar-assisted control," *Journal of Atmospheric and Oceanic Technology*, vol. 30, no. 10, pp. 2233 – 2240, 2013.

[14] W. H. Lio, A. Li, and F. Meng, "Real-time rotor effective wind speed estimation using Gaussian process regression and Kalman filtering," *Renewable Energy*, vol. 169, pp. 670–686, 2021.

[15] A. K. Pamososuryo, F. Spagnolo, and S. P. Mulders, "Analysis and calibration of optimal power balance rotor-effective wind speed estimation schemes for large-scale wind turbines," *Wind Energy Science*, vol. 10, no. 5, pp. 987–1006, 2025.

[16] J. Blank and K. Deb, "Pymoo: Multi-objective optimization in Python," *IEEE Access*, vol. 8, pp. 89 497–89 509, 2020.

[17] J. Aho, A. Buckspan, J. Laks, P. Fleming, Y. Jeong, F. Dunne, M. Churchfield, L. Pao, and K. Johnson, "A tutorial of wind turbine control for supporting grid frequency through active power control," in *2012 American Control Conference*, Montreal, QC, Canada, June 2012, pp. 3120–3131.

[18] R. Damiani, S. Dana, J. Annoni, P. Fleming, J. Roadman, J. van Dam, and K. Dykes, "Assessment of wind turbine component loads under yaw-offset conditions," *Wind Energy Science*, vol. 3, no. 1, pp. 173–189, 2018.